POLİTEKNİK DERGİSİ

JOURNAL of POLYTECHNIC

ISSN: 1302-0900 (PRINT), ISSN: 2147-9429 (ONLINE)
URL: http://dergipark.org.tr/politeknik

Mosaic defect and AFM study on GaN/AlInN/AlN/Sapphire HEMT structures

GaN/AlInN/AlN/Sapphire yapılar için mozaik kusur ve AFM çalışması

Yazar(lar) (Author(s)): *Ahmet Kürşat BİLGİLİ[1], Erkan HEKİN[2], Mustafa Kemal ÖZTÜRK[3], Süleyman ÖZÇELİK[4], Ekmel ÖZBAY[5]*

ORCID[1]: 0000-0003-3420-4936

ORCID[2]: 0000-0003-1661-3234

ORCID[3]: 0000-0002-8508-5714

ORCID[4]: 0000-0002-3761-3711

ORCID[5]: 0000-0003-2953-1828

Bu makaleye şu şekilde atıfta bulunabilirsiniz(To cite to this article): Bilgili A. K., Hekin E., Öztürk M. K., Özçelik S., Özbay E., "Mosaic defect and AFM study on GaN/AlInN/AlN/Sapphire HEMT structures ", ***Politeknik Dergisi***, 25(4): 1613-1619, (2022).

Erişim linki (To link to this article): http://dergipark.org.tr/politeknik/archive

DOI: **10.2339/politeknik.787700**

Mosaic Defect and AFM Study on GaN/AlInN/AlN/Sapphire HEMT Structures

Highlights

- *A detailed mosaic defect study is made on GaN/AlInN/AlN/Sapphire structure*
- *A detailed AFM study is made on GaN/AlInN/AlN/Sapphire HEMT structure*

Graphical Abstract

In this study, mosaic defect and detailed AFM investigation of GaN/AlInN/AlN/ Sapphire HEMT structure is made.

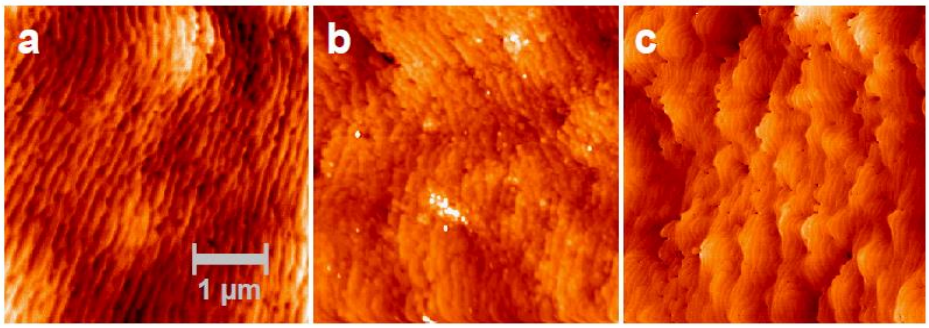

Figure. 5 AFM images of samples A, B and C

Aim

Aim of this study is to investigate mosaic defects and morphological properties of GaN/AlInN/AlN/sapphire HEMT structure.

Design & Methodology

Samples in this study are grown by metal organic chemical vapor deposition technique and XRD and AFM investigation is made on them.

Originality

This study is original because investigation of GaN/AlInN/AlN/Sapphire structure in such way is rare.

Findings

In this study dislocation density and surface properties of GaN/AlInN/AlN/sapphire structures are determined.

Conclusion

Dislocation densities, RMS values and twist angles are in good accordance with optimisation order of samples.

Declaration of Ethical Standards

The author(s) of this article declare that the materials and methods used in this study do not require ethical committee permission and/or legal-special permission.

Mosaic Defect and AFM Study on GaN/AlInN/AlN/Sapphire HEMT Structures

Research Article

Ahmet Kürşat BİLGİLİ[1*], Erkan HEKİN[2], Mustafa Kemal ÖZTÜRK[2], Süleyman ÖZÇELİK[2], Ekmel ÖZBAY[3]

[1]Science Faculty, Physics Department, Gazi University, Turkey
[2]Photonics Research and application center, Gazi University, Turkey
[3]Science Faculty, Physics Department, Bilkent University, Turkey

(Geliş/Received : 29.08.2020 ; Kabul/Accepted : 13.07.2021 ; Erken Görünüm/Early View: 03.08 2021)

ABSTRACT

In this study, three samples of GaN/AlInN/AlN/Al_2O_3 high electron mobility (HEMT) structures are investigated with high resolution X-ray diffraction (HR-XRD) technique. Peak positions and peak broadenings are used in calculations, gained from rocking curves. Structural quality is determined from symmetric and asymmetric peak planes. Mosaic defects such as treadening dilocations (TDs), tilt and twist angles, lateral and vertical crystallite lengths are determined by using Williamson Hall (WH) method. In addition to these, surface morphology is also investigated by atomic force microscopy (AFM). It is noticed that crystal quality of epitaxial layers decrease in the order of samples C, B and A. Al compositions for samples A, B and C are found as %87.4, %86.6 and %86.4, respectively by using Vegard's law.

Keywords: GaN, AlInN, AlN, sapphire, HEMT.

GaN/AlInN/AlN/Safir HEMT Yapılar için Mozaik Kusur ve AFM Çalışması

ÖZ

Bu çalışmada GaN/AlInN/AlN/Al_2O_3 yüksek elektron mobiliteli transistör (HEMT) yapıları üç numune olacak şekilde, yüksek çözünürlüklü X-ışınları kırınımı (HR-XRD) tekniği ile incelendi. Hesaplamalarda roking eğrilerinden elde edilen pik pozisyonları ve pik genişlemeleri kullanıldı. Yapısal kalite simetrik ve asimetrik pik düzlemlerinden faydalanılarak belirlendi. Tedirgin edici dislokasyonlar (TDs), eğim ve burkulma açıları, yanal ve düşey kristal uzunlukları gibi mozaik kusurlar Wiiliamson Hall (WH) metodu kullanılarak saptandı. Bunlara ilave olarak, yüzey morfolojisi atomik kuvvet mikroskopisi (AFM) yöntemiyle belirlendi. Epitaksiyel tabakaların kristal kalitesinin örnek C, B ve A sırasına göre düştüğü farkedildi. Örnekler A, B ve C için Al kompozisyonlarının sırasıyla %87.4, %86.6 ve %86.4 olduğu Vegard yasası kullanılarak belirlendi.

Anahtar Kelimeler: GaN, AlInN, AlN, safir, HEMT.

1. INTRODUCTION

AlGaN/GaN and AlInN/GaN based high electron mobility transistors (HEMTs) take great attention for high frequency, high power and micro wave applications in recent years. Because, nitrite based material systems have unique properties such as wide band gap and continuous piesoelectric polarisation field[1, 2, 3]. One of the most studied structure is electron gas (2DEG) coming out in hetero interface with continuous polarisation and AlGaN/GaN structure[4, 5]. Some succesful results are gained in AlInN GaN/GaN HEMTs by optimising growth parameters. For instance, at AlGaN/GaN interface, forming a thin AlN layer increase carrier density, decrease 2DEG alloy scattering and maintains formatting of carriers[3, 4].

Aliminium content that can be adjusted with great percentage gives hand to increase polarisation that cause charge density and carrier formatting in channel. Advantage of using AlInN buffer layer is, desinger can acquire good lattice and polarisation match by adjusting components of heterostructure. If In ratio is adjusted as %18 GaN lattice is in good accordance with substrate. Polarisation charge is described as continuous polarisation. Because piesoelectric polarisation of structure is zero. HEMTs with AlInN buffer layers are produced for gaining higher carrier density than HEMTs with AlGaN buffer layer. If mobility of latter is kept in the same level with the first, AlInN based device has better performance and this results with operating at high power and frequency.

There are many difficulties in epitaxial growth of AlInN based structures. Growth of AlN and InN requires different temperatures. Growth of AlInN is not easy by controlling alloy ratio. Number of studies on AlInN and AlInN/GaN hetero-structures is increasing rapidly in literature[4]. As a result of such succesful studies there are applications of AlInN HEMT structures[4]. The main advantage of AlInN/GaN hetero-structures is they have high interface sheet carrier density. Sheet carrier density

*Corresponding Author
e-mail: ahmet.kursat.bilgili@gazi.edu.tr

formed with continuous and piesoelectric polarisation overlaps the possible value for AlGaN/GaN. HEMT structure can be grown on traditional substrates.

The difference between thermal expansion coefficients of sapphire and GaN and AlN layers and lattice mismatch between them results with dislocation density as high as 10^8-10^{10} cm^{-2}. These dislocations effect defect structure of AlInN HEMTs. For this reason, GaN and AlN epitaxial films are frequently grown as mosaic blocks. They are characterised in relation with high density threadening dislocations (TDs) and with tilt and twist angles. These defected crystal structures effect device performance and life in great percentage[5]. HEMT device with its complex structure shows similarities with structures containing GaN and AlN buffer layers in terms of defects. HEMTs with AlN and GaN buffer layers have great potential in industrial production. Many researchers studied for minimising defects of them[5, 6]. For example, defect analysis, tilt and twist angles, dislocation density values of layers are determined by using symmetric and asymmetric peak broadening[7, 8]. In general, it is sufficient to determine full width at half maximum (FWHM) of a symmetric plane reflection. To investigate defects of HEMT device with AlInN layer with HRXRD, growth conditions should be optimised. In literature several studies take attention with tilt and twist angles gained experimentally[8, 9].

In this study AlInN (HEMT) samples are investigated. Samples are grown on c-oriented sapphire by using metal organic chemical vapor deposition method (MOCVD). Interface and surface structure of the samples are investigated by high resolution X-ray diffraction (HRXRD) and atomic force microscopy (AFM). Mosaic defects are investigated in detail by using these two techniques. Defected AlN and GaN layers of HEMT structure, edge and screw type dislocations, average tilt and twist angles, lateral and vertical mosaic crystal size are characterised. Symmetric (00.l) reflections and rocking curves are used to define tilt angle. Twist angle is determined by using asymmetric (hk.l) reflections and w scans. Also, mosaic structure is analysed dependent on indium ratio for (12.1) crystal orientations.

2. EXPERIMENTAL

AlN, AlInN and GaN layers are grown on (00.l) oriented sapphire substrate with MOCVD method. Trimethylgallium (TMGa), Trimethylindium (TMIn), Trimethylalliminium (TMAl) and amonia (NH_3) sources are used with Ga, Al and N. Hydrogen is used as carrier gas. Before growth of epitaxial film, in order to remove impurities on the surface, sapphire substrate is annealed at 1100 ^oC temperature for 10 minutes. AlInN HEMT structures are called as sample A, B and C respectively. Schematic diagram of samples are shown in Figure 1. Sample A has sapphire substrate, AlN nucleation layer and AlN buffer layer. During growth of this sample first 15 nm thick Al nucleation layer is formed at low temperature (840 ^oC). Later, reactor temperature is increased to 1150 ^oC to grow 500 nm thick AlN buffer layer. Sample B contains sapphire substrate, AlN nucleation layer, AlN and GaN buffer layers. For sample C, first 15-20 nm thick Al nucleation layer is grown at low temperature (840 ^oC). Later, reactor temperature is increased to 1150 ^oC and 600 nm thick AlN buffer layer is grown. As the last step, in order to maintain growth conditions of GaN layer, growth operation is stopped for 2 minutes. GaN buffer layer is grown with 2 µm thickness in 2 µm/hour growth rate at high temperature (1070 ^oC).

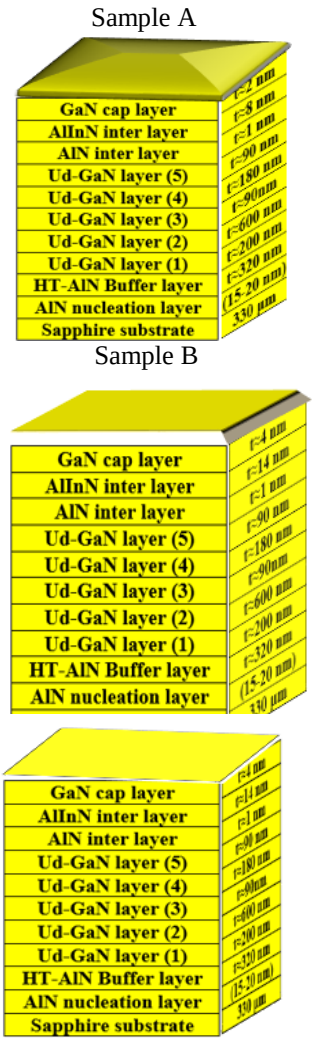

Figure 1. Schematic diagrams of samples A, B and C

3. RESULTS AND DISCUSSION

X-ray diffraction measurements of HEMT samples is performed with D8-Discovery high resolution diffractometer. This diffractometer have a goebel mirror and Ge (220) symmetric monocromator with 1.540 Å wavelength radiation. Peak positions and peak broadening of AlN and GaN films are gained from rocking curves. In order to present wurtzite hexagonal structure quality of HEMT samples HRXRD reflections of symmetric and asymmetric peak planes are used. Surface properties of samples are characterised with atomic force microscope (AFM). Symmetric and

asymmetric peak positions and peak FWHM values are presented in Table 1. In Table 1, peaks with no XRD resolution are shown as '-'.

AFM scans are made with Omicron VT-STM/AFM system in needle mode. Measurements are made on 4 μm^2 square region. Root mean square (RMS) roughness values are gained with Scala Pro software on surface topography mode.

In Figure 2 high resolution diffraction peaks for samples A, B, C can be seen. Three basic peaks gained from symmetric (00.2) plane are Bragg reflections for GaN buffer layer, InGaN barrier layer and AlN buffer layer.

Thickness of AlInN layers are determined from interference peak angles between AlInN and GaN by using semi-experimental X-ray wavelength equation. Calculated thickness values are 8.87, 6.5 and 10.76 nm respectively. Shoulders in peaks of GaN and AlN in all three samples may stem from non-stoichoimetric growth.

FWHM and peak positions of layers are given in Table 1. If these values are compared it can be seen that crystal quality of epitaxial layers decrease in order of samples A, C and B those contain GaN interlayer. If FWHM values of samples containing AlN interlayer are compared, it can be seen that crystal quality of epitaxial layers decrease in the order of samples C, B and A. Crystal quality of all three samples are approximately in the same tendency of change.

In and Al compositions in samples A, B and C are calculated with a convenient software. Results are shown in Figure 3.

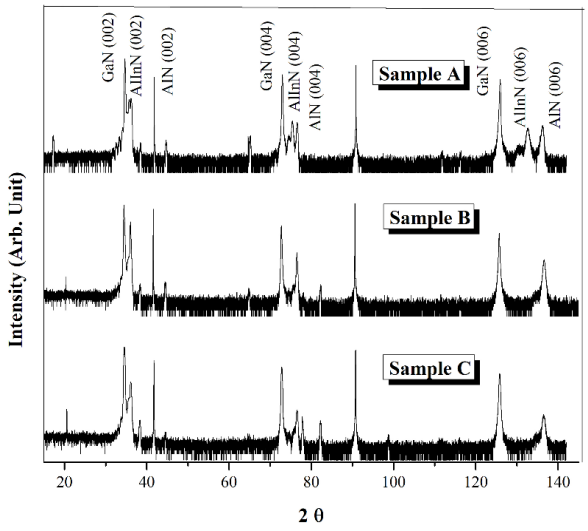

Figure 2. Bragg reflections of samples A, B and C on (00.2) plane.

Al compositions for samples A, B and C are found as %87.4, %86.6 and %86.4, respectively by using Vegard's law. $(x=c_{AlInN}-c_{InN})/(c_{AlN}-c_{InN})$. In HEMT structures, nitrite alloys such as GaN, AlN and AlInN have hexagonal structures. Quality of HEMT structures are measured with broadening of symmetric and asymmetric peaks. Broadening of symmetric and asymmetric rocking curves in GaN and AlN layers stems from tilt, twist angles and mosaic length parallel to surface of wafer. In Figure 3, FWHMs of symmetric (00.2) and (00.4) diffraction peaks for buffer and active layers versus In ratio can be seen. In increasing In ratio values FWHM of GaN layers are similar to each other in (00.2) and (00.4) planes. For larger FWHMs, AlN (00.4) and GaN shows similarity. AlN (00.2) presents opposite behaviour according to AlN (00.4) and GaN (00.2), (00.4). FWHM value for AlN (00.4) presents decreasing behaviour with increasing In ratio. Dependency of FWHM values versus In ratio can clearly be seen in Figure 3.

FWHM values of Φ decrease with increase of χ but FWHM values of w scans makes them increase. Thus, in χ at 78.6 º (12.1) reflection of all scans gives better FWHMs. In fact, when reflection plane is normal to surface of sample it reaches 90 º. These results are near to twist angles, width of rocking curves, for larger χ angles. In every terms, FWHM of Φ angles are bigger according to w- scans with tilt angle variation. For this reason at 78.6 º, twist angle should be average FWHM values for w and Φ scans. Twist angle values are found as 0.23 º, 0.16 º, 0.14 º for GaN layers of samples A, B and C respectively.

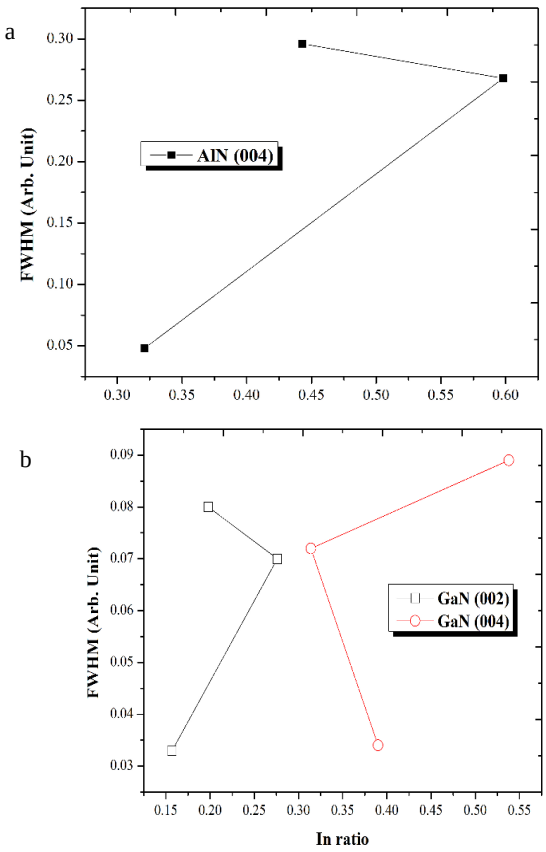

Figure 3. Variation of FWHM versus In ratio in AlN and GaN layers.

As In ratio increase, twist angles decrease. Similar to these, twist angle values for AlN layers are calculated

from (12.1) rocking or Phi scan FWHMs. They are determined as 0.28 º, 0.33 º and 0.16 º for samples A, B and C respectively.

Twist angle values for AlN layer first increase later decrease with increasing In ratio. In addition to this, twist angles for AlInN layer are not determined because HR-XRD peaks for (12.1) plane are not distorted. In symmetric diffraction geometry of HEMT structure, lateral lengths and tilt angle causes broadening of rocking curves. Contribution of these two effects causes linear dependency by broadening in reflection degree. This situation is used to seperate two effects from each other. A Williamson –Hall (WH) plot can be used for this aim. These plots are linear that are drawn using FWHM as a function of reflection degree. In Figure 4, FWHM (sinθ)/λ versus (sinθ)/λ is plotted. FWHM is the width of the measured peak at half maximum. λ and θ are wavelength of X-ray and incidence angle respectively. Tilt angle is determined by the slope of WH linear plot. Inverse of intercept point of this linear plot gives lateral mosaic length. Tilt and lateral mosaic length values are presented in Table 2. With increasing In content tilt angle values for GaN first increase later decrease. The same value for AlN layers presents a decreasing behaviour. At the same time, for GaN layer, lateral mosaic length first decrease later increase. Lateral mosaic length of AlN layer first increase later decrease. On the other hand, lateral mosaic blocks have less value than AlN layer.

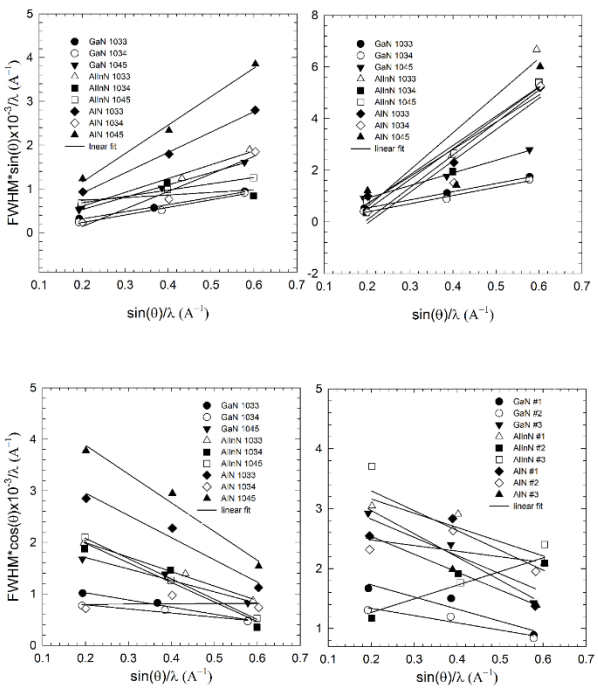

Figure 4. Williamson Hall plots for Sample A(1033), Sample B(1034), Sample C(1045).

	S.A		***S.B***		***S.C***	
GaN	Peak pos.	FWHM	Peak Pos.	FWHM	Peak Pos.	FWHM
(00.2)	17.380	0.080	17.407	0.033	17.352	0.070
(00.4)	36.537	0.089	36.568	0.034	36.596	0.072
(00.6)	63.083	0.068	-	-	63.063	0.077
(10.2)	24.047	0.208	24.057	0.248	24.056	0.228
(10.4)	-	-	53.600	0.080	-	-
(10.5)	52.500	0.264	-	-	52.507	0.098
(10.6)	68.990	0.253	76.460	0.594	69.042	0.096
(11.2)	34.645	0.349	34.773	0.260	34.673	0.246
(12.1)	48.892	0.368	48.954	0.284	48.950	0.250
AlN						
(00.2)	18.065	0.330	-	-	18.229	0.255
(00.4)	38.380	0.296	38.440	0.048	38.340	0.268
(00.6)	68.520	0.302	-	-	68.226	0.295
(10.2)	24.056	0.228	24.057	0.248	24.890	0.450
(10.4)	-	-	-	-	-	-
(10.5)	55.756	0.948	55.659	0.777	55.500	0.377
(10.6)	68.908	0.220	69.064	0.082	68.836	0.086
(11.2)	34.686	0.406	0.636	0.264	35.739	1.252
(12.1)	48.892	0.368	48.930	0.442	48.942	0.260
AlInN						
(00.2)	17.703	0.288	-	-	17.739	0.037
(00.4)	37.420	0.304	37.567	0.080	37.408	0.270
(00.6)	-	-	-	-	63.489	0.083
(10.2)	23.946	1.926	-	-	-	-
(10.4)	-	-	-	-	-	-
(10.5)	55.50	0.987	-	-	54.026	0.345
(10.6)	-	-	-	-	-	-
(11.2)	34.826	0.423	-	-	-	-
(12.1)	-	-	-	-	-	-

Table 1. Peak positions and FWHM values for Samples A, B and C.

Table 2. Mosaic properties of Sample A, B, C

GaN/AlN	**Lateral CL ($x10^3$)**	**Vertical CL($x10^3$)**	**Tilt($x10^{-3}$)**	**Screw ($x10^4/10^5$)**	**Edge ($x10^8/10^9$)**
	nm	nm	degree	cm^{-2}	cm^{-2}
A	3.2/0.3	0.4/0.8	0.9/5.7	1.67/208	2.9/12.5
B	1.2/23	1.6/1.6	2.2/1.1	13.9/4.2	89/0.7
C	4.6/9.1	0.7/0.3	1.2/1.3	0.41/5.4	15.7/2.4

In sample A, there is an opposite behaviour. The reason for this situation is decreasing size of mosaic blocks because of rapid cooling of sample during growth. Vertical mosaic block length normal to surface of wafer causes broadening of Bragg reflections in symmetric radial reflections with mixed strain along c-axis. In Figure 4, y-axis intercept point of linear plot is used in $L_{\perp}=0.9/2y_0$ to determine vertical mosaic block length. Strain is determined directly by the slope of these lines. Vertical mosaic lengths and heterogen starin values are presented in Table 2. Vertical mosaic lengths for GaN and AlN first decrease later increase. Also, for GaN layer vertical mosaic length value presents an opposite behaviour with lateral mosaic length but AlN has similar properties for both lateral and vertical mosaic lengths.

As it is known, wafers with lattice mismatch, such as Al_2O_3, SiC and Si, are difficult to use with hexagonal layers as GaN and AlN because they present high dislocation density. In this study, InGaN/GaN/AlN epilayers are grown on sapphire that results with high dislocation density. In order to see defects caused from crystallity level and mosaic block structure D_{edge} and D_{screw} type dislocation densities may be calculated wih equations (1) and (2) [7-9].

$$D_{edge} = \frac{\beta^2}{9b^2_{edge}} \quad (1)$$

$$D_{screw} = \frac{\beta^2}{9b^2_{screw}} \quad (2)$$

FWHM is measured wih HR-XRD rocking curves and it determines crystallity condition of samples. *b* is the lenght of Burgers vector. (For GaN, b_{screw}=0.5185 nm, b_{edge}=0.3189 nm and for AlN, b_{screw}=0.49792 nm, b_{edge}=0.31114 nm). Mixed type dislocation density for InGaN epilayer and GaN layers are calculated with equation (3).

$$D_{mix.} = D_{edge} + D_{screw} \quad (3)$$

Table 3. Dislocation densities for GaN and AlN

	Screw DL (GaN)x10^7	Screw DL (AlN) x10^8	Edge DL (GaN) x10^9	Edge DL (AlN) x10^9
S.A	7.87	2.88	2.21	1.00
S.B	9.11	1.02	3.65	0.32
S.C	0.62	0.12	0.98	0.02

Table 3 shows edge, screw type dislocation densities. In GaN layer, screw and edge type dislocation densities first increase later decrease in seventh degree. In AlN layer, both dislocation densities presents a decreasing behaviour. A second method for edge and screw type dislocation densities is dependent on Burgers vector, tilt angle and lateral mosaic length. All type of dislocations are dependent on lateral mosaic length, tilt and twist angles. For GaN (00.2) oriented epitaxial films, average twist angle is related with dislocation density with (*b=1/3*(11.0)) burgers vector. Also, average tilt angle is related with screw type dislocation density with *b*=(00.1) Burgers vector. Screw type dislocation density can be calculated with equation (4).

$$N_{screw} = \frac{\alpha^2_{(tilt)}}{4.35\left|b^2_{screw}\right|} \quad (4)$$

Here, α_{tilt} is tilt angle and *b* is the length of burgers vector. Edge type dislocation with (*b=1/3* (11.0)) Burgers vector, comes together with azimutual rotation of crystal around normal of surface. Edge type dislocation density can be calculated by measured twist angle[8-10]. If dislocations are gathered in grain boundaries, edge type dislocation density can be calculated with equation (4). Here peak broadening of asymmetric planes are length of Burgers vector and lateral mosaic length. As can be seen in Table 3 edge type dislocation densities are greater than screw type dislocation density by one degree. Dislocation movement results with plastic deformation. In an edge type dislocation, localised lattice deterioation is present along end of semi-plane of atoms. As edge type dislocations move with shear strain, movement of screw type dislocation results with shear strain and shear deformation. In crystals, characteristic structure of a wide angle grain boundary is distorted with a thin amorphous region. In grain boundary, atom dislocation results with discontunity in shift plane. For this reason, if dislocation is stopped by grain boundary and there occurs stacks. If particle size is smaller, dislocations are gathered more frequently. For all three samples, screw type dislocation density decrease in fourth degree. Also, edge type dislocation density first decrease later increase in nineth degree. Edge type dislocation density is larger than screw type dislocation density in approximately one degree. Variation of dislocation density for AlN layer is similar to variation in GaN layer but AlN layers have larger dislocation densities in general.

Surface morphology of III-nitrite mixed structures effects performance of HEMT device. In Figure 5. AFM images gained from GaN cap layer of AlInN HEMT samples in 4x4 μm^2 scanning area can be seen. As can be seen in Figure 5, samples A and B have similar surface morphology, they both have steps and terraces. In sample C, in opposition with common clean atomic steps, there are dark dots[11, 12]. Different surface morphology of samples is related with thickness of AlInN layer and GaN cap layer. Root mean square (RMS) values for samples A, B and C in 4x4 μm^2 area are 0.46, 0.28 and 0.56 nm respectively. Results imply that, terrace width of GaN cap layers are in good accordance RMS values. RMS values of sample C are higher than other two samples,

this situation may stem from narrow steps on the surface and dark dot difference. In addition to these, most of dark dots are turned into island-like structure from terrace structure in the image of sample C in Figure 5.

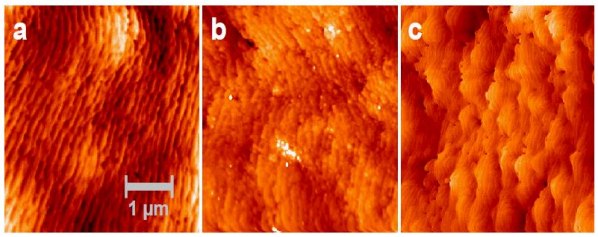

Figure 5. AFM images of samples A, B and C

As far as it is known, end of steps are dependent on screw or mixed type dislocations[10-13]. In sample C end of step density in 4x4 μm^2 scanning area is approximately $1.06x10^9$ cm^{-2}. AFM images show that surface morphology of samples are strongly dependent on In content. As In content increase, surface morphology changes as island-like.

CONCLUSION

In this study, three samples of GaN/AlInN/AlN/Al_2O_3 high electron mobility (HEMT) structures are investigated with high resolution X-ray diffraction (HR-XRD) technique. TD values of the samples are found around 10^8-10^{10} cm^{-2}. Thickness values are calculated around 8.87, 6.5 and 10.76 nm for samples A, B and C respectively. Crystal quality of the samples are determined in the order of samples A, C and B. Al compositions are determined as %87.4, %86.6 and %86.4 for samples A, B and C respectively by using Vegard's law. Twist angle values for GaN layer are 0.23º, 0.16º, 0.14º and for AlN layer the same values are as 0.28º, 0.33º and 0.16º for samples A, B and C. RMS values from AFM scans are determined as 0.46, 0.28, 0.56 nm for samples A, B and C. AFM images show that surface morphology of samples are strongly dependent on In content. As In content increase, surface morphology changes as island-like. Results gained in this study are in good accordance with previous works done by different researchers.

ACKNOWLEDGEMENT

This work was supported by Presidency Strategy and Budget Directorate (Grant Number: 2016K121220).

DECLARATION OF ETHICAL STANDARDS

The author(s) of this article declare that the materials and methods used in this study do not require ethical committee permission and/or legal-special permission.

AUTHORS' CONTRIBUTIONS

Ahmet Kürşat BİLGİLİ: Performed the experiments and analyse the results.

Erkan HEKİN: Performed the experiments and analyse the results.

Mustafa Kemal ÖZTÜRK: Wrote the manuscript.

Süleyman ÖZÇELİK: Maintained all technical opportunity for forming this article.

Ekmel ÖZBAY: Maintained necessary software for electronic work.

CONFLICT OF INTEREST

There is no conflict of interest in this study.

REFERENCES

[1] Vickers M. E., Kappers M. J., Datta R., McAleese C., Smeeton T. M., Rayment F., Humphreys C. J., "In-plane imperfections in GaN studied by x-ray diffraction", ***J. Phys. D: Appl. Phys***. 38, A99, (2005).

[2] Awual R., Asiri M., Rahman M., Alharthi H., "Assessment of enhanced nitrite removal and monitoring using ligand modified stable conjugate materials", ***Chemical Engineering Journal***, 363: 64-72.

[3] Zheng H., Chen H., Yan Z., Han Y., Yu H., Li D., Huang Q., Zhou J., "Determination of twist angle of in-plane mosaic spread of GaN films by high-resolution X-ray diffraction", ***J. Cryst. Growth*** 255, 63 (2003).

[4] Xing H., Keller S., Wu Y. F., McCarthy L., Smorchkova I. P., Buttari D.,Coffie R., Green D. S., Parish G., Heikman S., Shen L., Zhang N., Xu J. J., Keller B. P., DenBaars S. P., Mishra U. K., "Gallium nitride based transistors", ***J. Phys. Cond. Matt.,***13: 7139-7157 (2001).

[5] Dunn C. G., Koch E. F., "Comparison of dislocation densities of primary and secondary recrystallization grains of Si-Fe", ***Acta Metall***. 5: 548 (1957).

[6] Heikman S., Keller S., Wu Y., Speck J., DenBaars P., Mishra K., "Polarization effects in AlGaN/GaN and GaN/AlGaN/GaN heterostructures", ***Journal of Applied Physics*** 93, 10114.

[7] Çörekçi, S. Öztürk M. K., Bengi A., Çakmak M., Özçelik S., Özbay E.**,** "Characterization of an AlN buffer layer and a thick-GaN layer grown on sapphire substrate by MOCVD", ***J. Mater. Sci.*** DOI 10.1007/s10853-010-4973-7, (2010).

[8] S. Çörekçi., M. K. Öztürk., B. Akaoğlu., M. Çakmak., S. Özçelik., E. Özbay., "Structural, morphological, and optical properties of AlGaN/GaN heterostructures with AlN buffer and interlayer", ***J. Appl. Phys.*** 101, 123502, (2007).

[9] Çörekçi S., Usanmaz D., Tekeli Z., Çakmak M., Özçelik S., Özbay E., "Surface Morphology of Al0.3Ga0.7N/Al2O3-High Electron Mobility Transistor Structure", ***J. Nanoscience and Nanotechnology***. 8, 640-644, (2008).

[10] Ungár T., "Microstructural parameters from X-ray diffraction peak broadening", ***Scripta Materialia***, Volume 51, Issue 8, 2004, Pages 777-781,(2004).

[11] Nakamura N., Furuta K., Shen X., Kitamura T., Nakamura K., Okumura H., "Electrical properties of MBE-grown AlGaN/GaN HEMT structures by using 4H-SiC (0 0 0 1) vicinal substrates", ***Journal of Crystal Growth*** 301–302 452–456, (2007).

[12] Mahanty S., Hao M., Sugahara T., Fareed Q., Morishima Y., Naoi Y., Wang T., Sakai S., "V-shaped defects in InGaN/GaN multiquantum wells**",** ***Materials Letters*** 41, 67–71, (1999).

Kapolnek D., Wu X., Heying B., Keller S., Mishra U., DenBaars S., Speck J., " Structural evolution in epitaxial metalorganic chemical vapor deposition grown GaN films on sapphire"***, Appl. Phys***. ***Lett***. 67:1541-1543, (1995)